Chapter 7

Comparative study for removal of aqueous methylene blue using biochar from pyrolysis of raw and torrefied biomass: kinetics, isotherm, thermodynamics and mass transfer studies

General background

This chapter aimed to investigate the performance of biochars from pyrolysis of raw *Acacia nilotica* (Biochar-DAN) and torrefied *Acacia nilotica* (Biochar-TAN) towards removal of aqueous methylene blue (MB) dye using batch adsorption. Both biochars were characterized for physicochemical, BET surface area, SEM-EDX, FTIR and XRD analyses. Impact of time, adsorbent dose, pH, concentration of MB and temperature was examined. A detailed study of adsorption kinetics, isotherm, thermodynamics and mass transfer studies were performed. In addition, the possible mechanism for adsorption of MB onto biochar has been proposed.

7.1 Introduction

Over the last few decades, upsurge in the generation of contaminated water is witnessed due to rapid increase in population as well as industrialization (Güzel et al., 2017). Among various organic and inorganic toxic pollutants, synthetic dyes a kind of organic pollutant from several industries such as paint, textile, leather, paper, and cosmetics, etc. are common pollutant which are severely affecting the water bodies (Karoui et al., 2020; Lyu et al., 2018; Sangon et al., 2018). Methylene blue (MB), a type of cationic dye has vast application in textile dyeing industry, ink manufacturing industry and as an indicator (Mahmoud et al., 2012; Zhai et al., 2019). The MB present in wastewater is non-biodegradable due to its high toxicity and chemical stability (Mahmoud et al., 2012; Zhai et al., 2019). The MB concentration higher that 7 mg/kg can cause abdominal pain, mental disorder, high blood pressure and nausea to human body (Lyu et al., 2018). The treatment of contaminated water is prerequisite and rather imperative as it is imposing serious threat to the aquatic life cycle and creating imbalance to the environment due to its non-biodegradability and carcinogenic effect (Li et al., 2018; Liu et al., 2019; Rafatullah et al., 2010).

The adsorption has already been proven as an efficient and effective method for wastewater treatment, because of its lower operational cost and higher removal efficiency, rapid reaction rate, design and operational simplicity (Lyu et al., 2018; Mahmoud et al., 2012; Zhai et al., 2019), as per the acknowledgement given by the United States Environmental protection Agency (USEPA) (Lyu et al., 2018; Wanassi et al., 2017). In recent years, large number of adsorbents has been synthesized and their efficiency has been tested towards the removal of MB from wastewater. For instance, various type of activated carbon (Benhouria

et al., 2015), zeolites (Yang et al., 2018), and biochar are obtained from different thermochemical routes for instance gasification, pyrolysis, torrefaction, carbonization and hydrothermal of various carbonaceous materials. Nowadays, biochar has gathered huge attention in wastewater treatment processes because it is chemically stable and environmentally friendly (Lyu et al., 2018; Zhang et al., 2020). It is low cost, has high surface area, porosity, and higher carbon content (Trakal et al., 2014). High functionality of biochar surface imparts adsorption potential for toxic substances present in wastewater (Uchimiya et al., 2010). Biochar from thermochemical processes has also been chemically engineered to improve its adsorption capacity (Lyu et al., 2018). However, chemically treated biochars have certain limitations, such as cost and associated problems of release of chemicals (Lyu et al., 2018).

The integrated approach of torrefaction-pyrolysis process can enhance the quality of products (bio-oil, biochar and pyrolytic gases) from pyrolysis process (Dai et al., 2019). Being an energy intensive process, torrefaction can influence the overall economy of the pyrolysis process. Therefore, utilization of by-product such as biochar from integrated process may facilitate the overall economy of the process by making it cost effective. The efficacy of biochar obtained from pyrolysis of variety of native biomass samples as an adsorbent has been comprehensively investigated by various researchers as discussed in Chapter 2. However, studies comparing adsorption efficiency of biochar from pyrolysis of raw and torrefied biomass have not been reported for MB removal. Also, the application of biochar obtained at optimum condition of pyrolysis for maximum bio-oil yield has not been studied so far.

7.2 Material and methods

7.2.1 Material

The Biochar-DAN and Biochar-TAN were used as an adsorbent for the removal of MB dye. The detailed discussion availability, collection and preparation of DAN may be found in Chapter 3. All chemical reagents having analytical grade and methylene blue dye were procured from S.D. Fine-Chem Ltd. and Merck Chemical, India, were used with no further purification.

7.2.2 Experimental procedure for preparation of biochar from pyrolysis of DAN and TAN-252-60-5

The detailed discussion about experimental set-up has been given in Chapter 3. The detailed about the preparation of biochar (Biochar-DAN and Biochar-TAN) has been discussed in Chapter 6 where DAN and TAN has been used for pyrolysis process. The Biochar-DAN and Biochar-TAN were the biochar obtained at optimum condition of pyrolysis for maximum pyrolysis oil yield from pyrolysis of torrefied *Acacia nilotica*. The bio-oil yield was maximum at a temperature of 507 ℃, retention time of 58 min, heating rate of 38 ℃/min and sweeping gas flow rate of 40.52 mL/min.

7.2.3 Characterization of biochar obtained from pyrolysis of DAN and TAN-252-60-5

Proximate and ultimate analyses were performed to characterize Biochar-DAN and Biochar-TAN. The solid addition technique (Liu et al., 2016) was employed to determine

the point of zero charge on the surface of adsorbent (Biochar-DAN and Biochar-TAN) which signifies the net charge density on the surface of adsorbent. The Fourier Transform Infrared Spectroscopy (FTIR) was performed to classify the functional groups present in Biochar-DAN and Biochar-TAN before and after adsorption due to change in vibrational frequency. The surface characteristics such as morphology and elements exist on surface of Biochar-DAN and Biochar-TAN before and after adsorption were studied by Scanning Electron Microscopy (SEM) and Energy-Dispersive X-ray spectroscopy (EDX). The crystalline structure of Biochar-DAN and Biochar-TAN was explored with X-ray Diffraction (XRD) analysis. The XRD spectra were studied at ambient temperature with Cu-Kα monochromatic radiation in the 2θ ranging from 10-80° with 2°/min scanning rate. Table 7.1 represents the specification of various instruments used for characterization of biochar and batch adsorption process.

Table 7.1 Specification of various analytical instruments used for characterization of biochar and batch adsorption process

Analytical instruments	Specification
CHNS analyzer	EURO EA3000, EURO ITALY
FTIR analyzer	Model Varian 1000, USA
SEM-EDX analyzer	Model JEOL JSM5410, Japan
UV- Spectrophotometer	Model 2201, Systronics India
Shaking speed incubator	Model NSW-133, Calton New Delhi, India
pH meter	Model LI 120, Elico, India
BET surface area analyzer	ASAP 2020 Micromeritics, USA
X-ray diffraction analyzer	mini flux II, Rigaku, Japan

7.2.4 Experimental procedure for removal of MB by batch adsorption process

The batch mode adsorption was performed for treatment of aqueous MB solution via Biochar-DAN and Biochar-TAN as adsorbents. Desired quantity of adsorbent was added in 50 mL MB solution of specific concentration in a 100 mL conical flask maintained at fixed pH. The flask was agitated in an incubator at a speed of 150 rpm at 25 ℃ until it attained the equilibrium. After that, the solution was filtered and the supernatant was examined by spectrophotometer to investigate the residual concentration of MB. Table 7.2 represents the variation of different parameters which were studied during the batch adsorption process. The pH of dye solution at desired value was obtained by adjusting the solution with 0.1M HNO_3 and 0.1M KOH solution. Preparation of stock solution of dye, cleaning of flasks and dilution of stock solution to obtain desired concentration of dye solution was done by using double distilled water. The percentage removal of MB and adsorption capacity was obtained by employing Eqs. (7.1) and (7.2), respectively.

$$\% \text{ Removal} = \frac{C_o - C_e}{C_o} \times 100 \quad (7.1)$$

$$q_e = \frac{(C_o - C_e) \times V}{M} \quad (7.2)$$

where C_o and C_e is initial and equilibrium concentration of MB in mg/L. q_e is adsorption capacity of adsorbent in mg/g. V is volume of MB solution in litre (L) and M is mass of adsorbent dose in gram (g).

Table 7.2 Different experimental conditions and their ranges studied during batch adsorption of MB dye

S. No.	Parameters studied	Range of operating parameters				
		pH	Adsorbent dose (g/L)	Temperature (K)	Initial concentration of MB (mg/L)	Equilibrium time (min)
1	Initial pH	2-11	2	298	50	1200
2	Equilibrium time	10	2	298	50	0-1200
3	Adsorbent dose	10	0.2-6	298	50	200
4	Temperature	10	2	293-323	50	200
5	Initial concentration of MB	10	2	298	10-300	200

7.3 Results and discussion

7.3.1 Characteristics of adsorbent Biochar-DAN and Biochar-TAN

7.3.1.1 Proximate and ultimate analyses of Biochar-DAN and Biochar-TAN

The detailed discussion about proximate analysis, ultimate analysis and higher heating value of both biochar (Biochar-DAN and Biochar-TAN) has been given in Chapter 6.

7.3.1.2 Point of zero charge (pH_{pzc}) for Biochar-DAN and Biochar-TAN

The pH_{pzc} of adsorbent is a very crucial parameter to comprehend the adsorption mechanism. It may be defined as the value of pH of solution at which net charge density of adsorbent surface is zero. At a pH of solution lower than the pH_{pzc}, the surface of adsorbent will be mostly positively charged, while, at a pH of solution higher than the pH_{pzc}, the

surface of adsorbent will be mostly negatively charged (Ronix et al., 2017). The point of zero charge allows in predicting the range of pH in which the electrostatic attraction between adsorbate and adsorbent favors the adsorption process. The pH_{pzc} for Biochar-DAN and Biochar-TAN was found to be 8.1 and 7.6, respectively (Fig. 7.1). The lower value of pH_{pzc} in case of Biochar-TAN might be due to lower intensity of functional groups associated with it. Since, Biochar-TAN has been obtained from pyrolysis of TAN which is obtained by thermally treating the DAN during torrefaction.

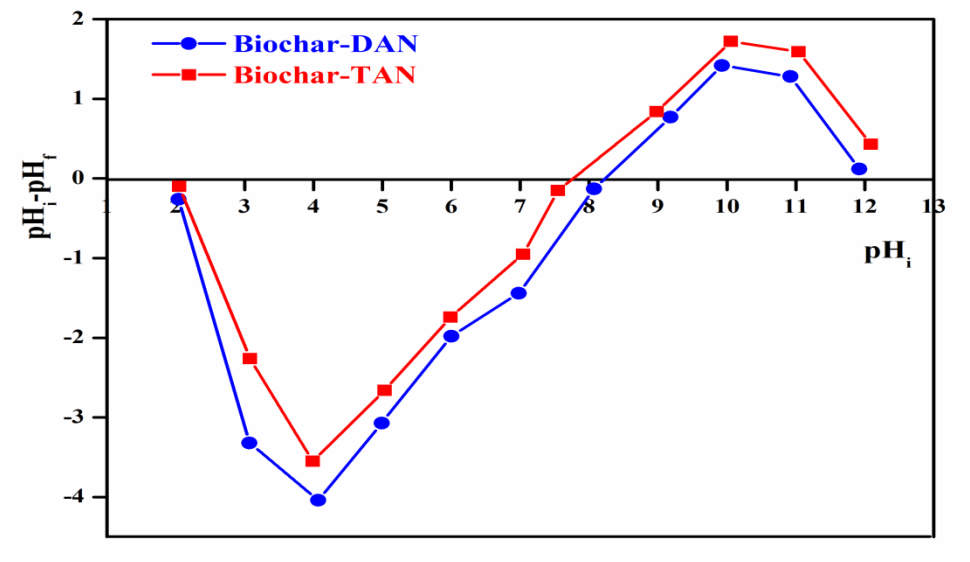

Figure 7.1 Point of zero charge (pH_{pzc}) for Biochar-DAN and Biochar-TAN

7.3.1.3 XRD analysis of Biochar-DAN and Biochar-TAN

Powder X-ray diffraction (XRD) analysis of Biochar-DAN and Biochar-TAN were performed. The results are shown in Fig. 7.2. It can be seen that broad peaks at 2θ value around 22^{o} in both the biochars corresponds to C(002). The C(002) plane was attributed to

parallel and azimuthal orientation of partially carbonized aromatic lamellae (Huang et al., 2009; Mohan et al., 2018). Broad and flat peaks for C(002) plane signifies lower degree of orientation (Huang et al., 2009).

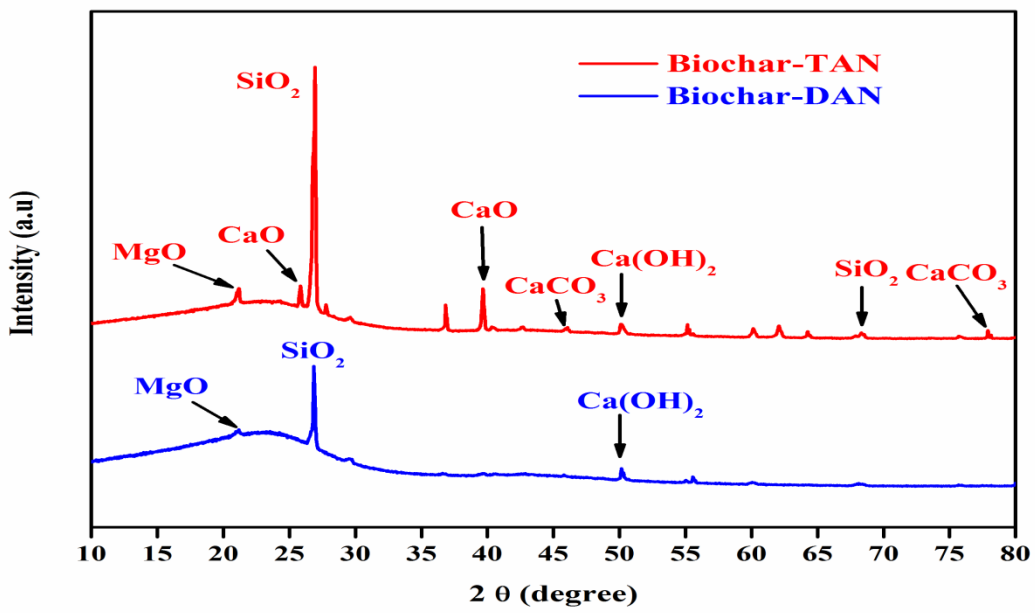

Figure 7.2 XRD analysis of Biochar-DAN and Biochar-TAN

Lui et al. (Liu et al., 2012) also concluded that broad peak between 2θ of 20^o and 30^o corresponds to staking structure of aromatic layer and broadening of peak arises due to small dimension of crystal perpendicular to aromatic layer. The Sharp and small peaks in case of Biochar-DAN at 2θ around 21^o and 50^o corresponds to MgO and $Ca(OH)_2$, while, a sharp and strong peak at 2θ around 27^o corresponds to SiO_2 (Mohan et al., 2018). In case of Biochar-TAN, more sharp and higher intensity peaks than the Biochar-DAN were identified at 2θ around 21^o, 26^o, 27^o, 39^o, 46^o, 50^o, 68^o, and 78^o which corresponds to MgO,

CaO, SiO_2, CaO, $CaCO_3$, $Ca(OH)_2$, SiO_2 and $CaCO_3$, respectively. Similar results can be found in published literatures (Huang et al., 2009; Liu et al., 2012; Mohan et al., 2018).

7.3.1.4 BET surface area and SEM-EDX analysis of Biochar-DAN and Biochar-TAN

The results of BET analysis are given in Table 7.3. The BET surface area of Biochar-DAN and Biochar-TAN was found to be 80.40 and 103.47 m^2/g, individually. The t-plot micropore volume of Biochar-DAN and Biochar-TAN was found to be 0.0641 and 0.0905 cm^3/g, respectively. Further, the BJH adsorption and desorption average pore diameter of Biochar-DAN and Biochar-TAN was noted to be 2.58 and 3.14 nm, and 2.13 and 2.87 nm, respectively. Both the biochars may be categorized as mesoporous material since their average pore size was found between 2 to 50 nm (Fan et al., 2017). Thus, results showed that both the biochar (Biochar-DAN and Biochar-TAN) can be potentially used as adsorbent; however, Biochar-TAN has superior properties than the Biochar-DAN for adsorption process.

Table 7.3 BET surface area analysis of Biochar-DAN and Biochar-TAN

Properties	Biochar-DAN	Biochar-TAN
BET surface area (m^2/g)	80.40	103.47
micropore volume (cm^3/g)	0.0641	0.0905
BJH adsorption average pore diameter (nm)	2.5881	3.1478
BJH desorption average pore diameter (nm)	2.1399	2.8709

Figs. 7.3(a) and (b) depict the SEM-EDX analysis of Biochar-DAN before and after adsorption. Fig. 7.3(a) depicts honeycomb like structure (Fan et al., 2017) of Biochar-DAN before adsorption where wide pores can be seen. EDX analysis confirmed that C, K, Ca, O, N were exist on the surface of Biochar-DAN. The pores present on the surface of Biochar-DAN facilitate its potential in adsorption process. The SEM-EDX analysis of Biochar-DAN after adsorption is depicted in Fig. 7.3(b), where blocked pores can be seen due to

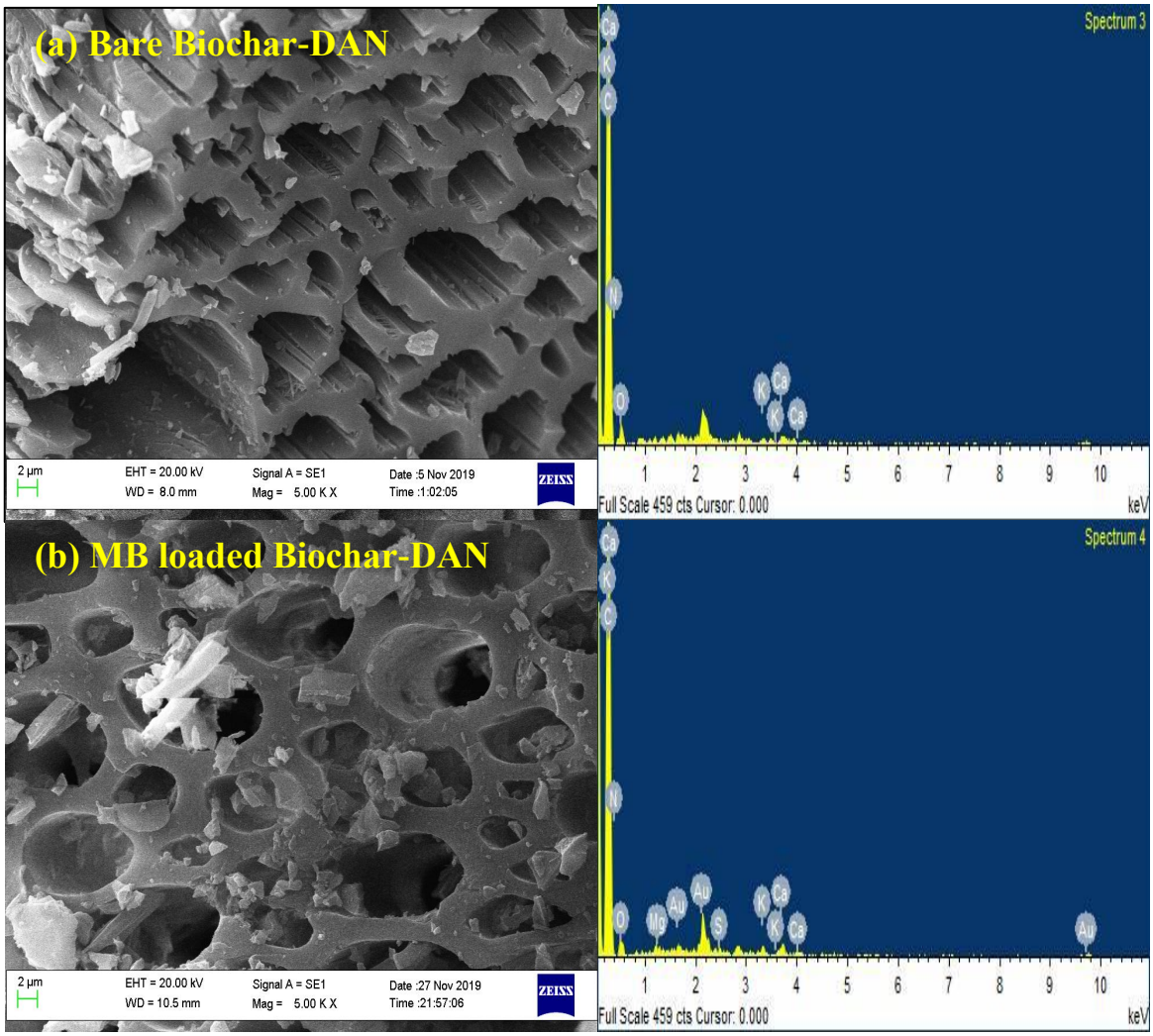

Figure 7.3 SEM-EDX analysis of Biochar-DAN before and after adsorption (a) Bare Biochar-DAN (b) MB loaded Biochar-DAN

layer of matter deposited inside the pores which confirmed the adsorption of MB on biochar. Element S along with C, K, Ca, O, N was perceived on the surface of biochar after adsorption which further confirmed the adsorption of MB.

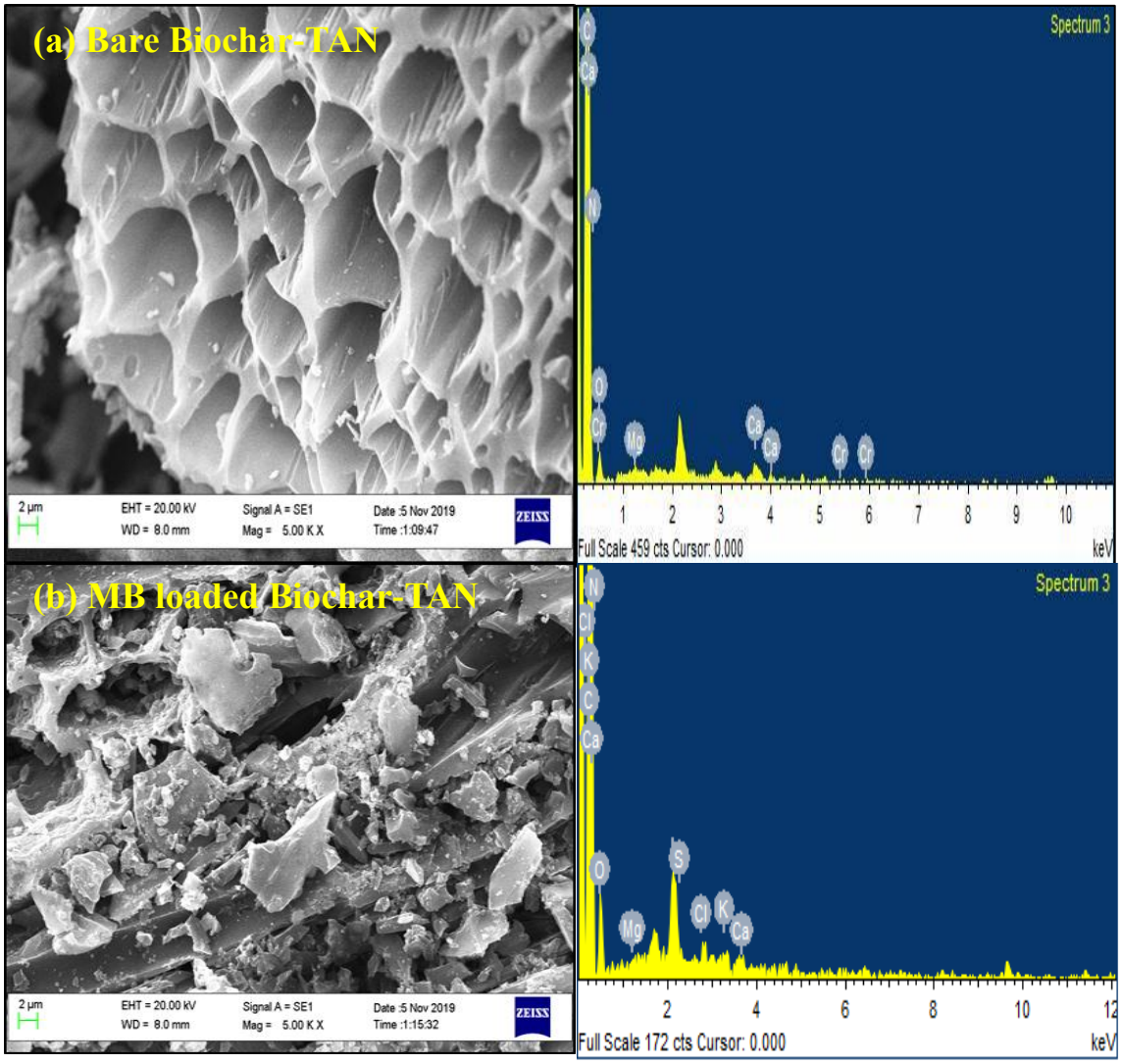

Figure 7.4 SEM-EDX analysis of Biochar-TAN before and after adsorption (a) Bare Biochar-TAN (b) MB loaded Biochar-TAN

Figs. 7.4(a) and (b) present the SEM-EDX of Biochar-TAN before and after adsorption. Biochar-TAN has wider pores than the Biochar-DAN. The EDX analysis confirmed that C, K, Ca, O, N, Mg were existing on the surface of Biochar-TAN. In case of Biochar-TAN after adsorption, filled pores can be seen. Element S and Cl can be seen in EDX image of Biochar-TAN suggesting the adsorption of MB on biochar.

7.3.1.5 FTIR analysis of biochar Biochar-DAN and Biochar-TAN

The FTIR analysis of Biochar-DAN and Biochar-TAN before and after adsorption was performed and their spectra are displayed in Fig. 7.5(a) and (b). The FTIR analysis provides a quick and efficient technique to identify the class of various chemical compounds. The FTIR spectra confirm the presence of various functional groups associated with biochar.

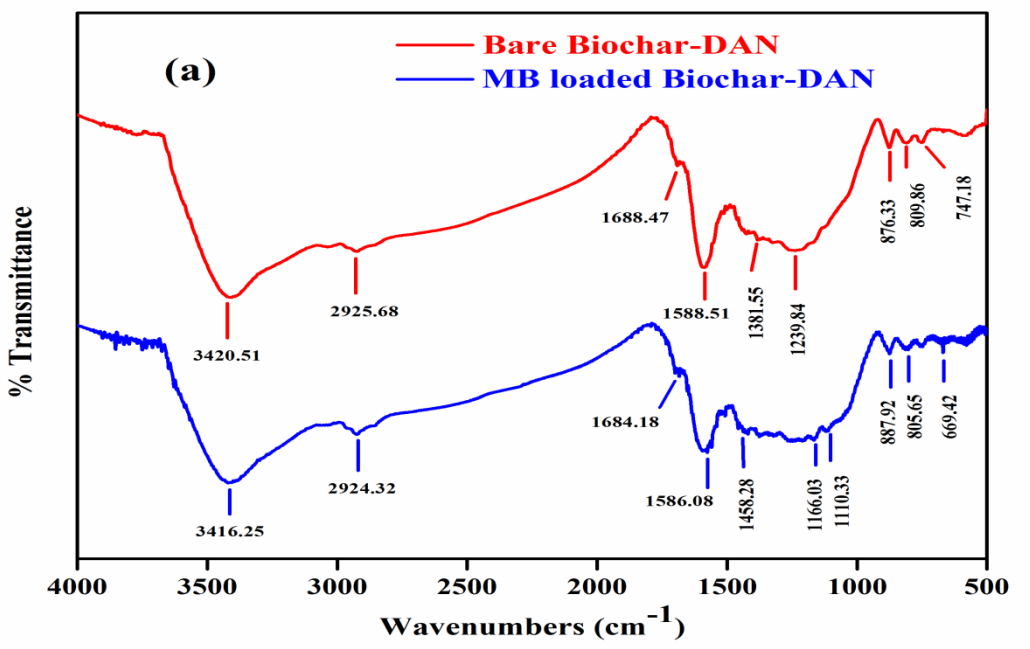

For Biochar-DAN, the peaks at 3420.51 cm^{-1} (before adsorption) and 3416.25 cm^{-1} (after adsorption) correspond to stretching vibration of O-H bonded groups such as phenol,

alcohol, and water (Fan et al., 2017). The wavenumbers 2925.68 cm^{-1} (before adsorption) and 2924.32 cm^{-1} (after adsorption), are ascribed to the stretching and deformation vibration of aliphatic C-H groups. The wavenumbers 1688.47 cm^{-1} (before adsorption) and 1684.18 cm^{-1} (after adsorption) are assigned to C=O vibration of aldehyde, and ketones and C=C aromatic vibrations. The wavenumbers 1588.47 cm^{-1} (before adsorption) and 1586.18 cm^{-1} (after adsorption) correspond to secondary amine groups. The wavenumbers 1239.84 cm^{-1} (before adsorption) and 1166.03 cm^{-1} (after adsorption) are ascribed to deformative vibration of aromatic nitrogen to secondary amine groups. The wavenumber between 876.33- 805.65 cm^{-1} and 757.12-686.51 cm^{-1} ascribe the presence of wagging vibration of C-H bond in aromatic ring and vibration of alkyl halide along with bending vibration of Si-O-Si bond, respectively (Chen et al., 2019).

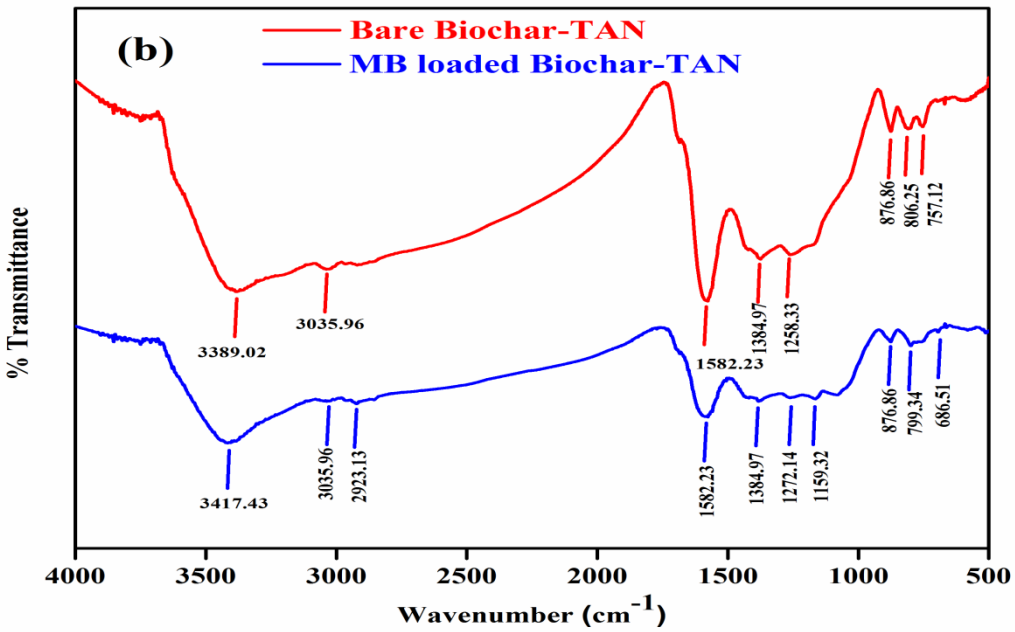

Figure 7.5 FTIR analysis of Biochar-DAN and Biochar-TAN before and after adsorption (a) Bare and MB loaded Biochar-DAN (b) Bare and MB loaded Biochar-TAN

Similar results were obtained for Biochar-TAN as well. The detailed analysis of FTIR spectra and assignment of different wavenumber is presented in Table 7.4. The intensity for Biochar-TAN was slightly lower than that of Biochar-DAN. This might be due to torrefaction as considerable rupture of –C-O, -O-H etc. bonds takes place and there is formation of CO_2 and lighter non-condensable gases. The intensity of functional groups such as –O-H, -C-H, -N-H and -C=O decreased after adsorption of MB on the biochar. This confirmed that these groups have participated in adsorption process. Also, in case of Biochar-DAN, some wavenumbers such as 1381.55, and 747.18 cm^{-1} disappeared, while, some new wavenumbers such as 1458.28, 1110.3, and 669.42 cm^{-1} were identified. Similarly, in case of Biochar-TAN, 757.12 cm^{-1} disappeared, while wavenumber 2923.33, 1159.32, 686.51 cm^{-1} were identified. This might be due to chemisorption on the surface of biochar resulting in formation of new compounds (Ji et al., 2019). The formation of hydrogen bond between –OH group of biochar and oxygen present in MB and electrostatic attraction of cationic MB by large number of –OH groups present in the solution at higher pH are mainly responsible for adsorption of MB on the biochar. In addition, the functional groups having oxygen atoms also form complex with MB molecules through surface complexation resulting in adsorption of MB on the surface of biochar (Fan et al., 2017).

Table 7.4 Functional groups detected in Biochar-DAN and Biochar-TAN before and after adsorption of MB dye

Bare Biochar-DAN (wavenumber cm^{-1})	MB loaded Biochar-DAN	Diff	Assignment	Bare Biochar-TAN	MB loaded Biochar-TAN	Diff	Assignment
3420.51	3416.25	4.26	Bonded -OH groups	3389.02	3417.43	-28.41	Bonded -OH groups
2925.68	2924.32	1.36	Aliphatic C-H group	3035.96	3035.96	0	Aromatic C-H group
1688.47	1684.18	4.29	Assigned to C=O and C=C aromatic vibrations	-	2923.33	-	Aliphatic C-H group
1588.51	1586.08	2.43	Secondary amine groups	1582.23	1582.23	0	Assigned to C=O and C=C aromatic vibrations
1381.55	-	-	-CH bending, $-CH_3$ asymmetric bending	1384.97	1384.97	0	-CH bending, $-CH_3$ asymmetric bending
-	1458.28	-	C-H alkanes in aromatic ring	1258.33	1272.14	-13.81	Ar-N deformation vibration
1239.84	1166.03	73.81	Ar-N deformation vibration	-	1159.32	-	Ar-N deformation vibration
-	1110.3	-	Ar-N deformation vibration	876.86	876.86	-	Wagging vibration of C-H in aromatic ring
876.33	887.92	-11.5	Wagging vibration of C-H in aromatic ring	806.25	799.34	6.91	Wagging vibration of C-H in aromatic ring
809.86	805.65	4.21	Wagging vibration of C-H in aromatic ring	757.12	-	-	Alkyl halide, Bend vibration of Si-O-Si
747.18	-	-	Alkyl halide, Bend vibration of Si-O-Si	-	686.51	-	Alkyl halide, Bend vibration of Si-O-Si
-	669.42	-	Alkyl halide, Bend vibration of Si-O-Si	-	-	-	-

7.3.2 Batch adsorption analysis of MB onto Biochar-DAN and Biochar-TAN

7.3.2.1 Effect of contact time and initial concentration of MB

The contact time for adsorption has obvious effect on adsorption capacity of both biochars. Fig. 7.6(a) and Fig. 7.7(a) display the effect of contact time on adsorption capacity of MB for Biochar-TAN and Biochar-DAN, respectively. The adsorption capacity for both the biochar increased sharply up to first 200 min and then slowly attains stability before reaching to equilibrium. The rapid increase in uptake capacity at the beginning is attributed to fast diffusion of MB molecules from the liquid solution to external surface of adsorbent; while slow and steady uptake capacity after certain time owing to longer diffusion path to interior pores of adsorbent and saturation of active sites for further adsorption (Ji et al., 2019; Li et al., 2018). In addition, uptake capacity increased as the initial concentration of MB increased. At higher concentration of dye, the probability of effective collision between adsorbent and MB molecule increased, resulting in higher adsorption capacity (Alinejad-Mir et al., 2018; Banerjee & Chattopadhyaya, 2017). Furthermore, the adsorption capacity of Biochar-TAN was higher than the Biochar-DAN. This might be due to higher surface area, higher active sites, pore size and surface complexation due to higher concentration of calcium, magnesium and silicon ions on the surface of Biochar-TAN.

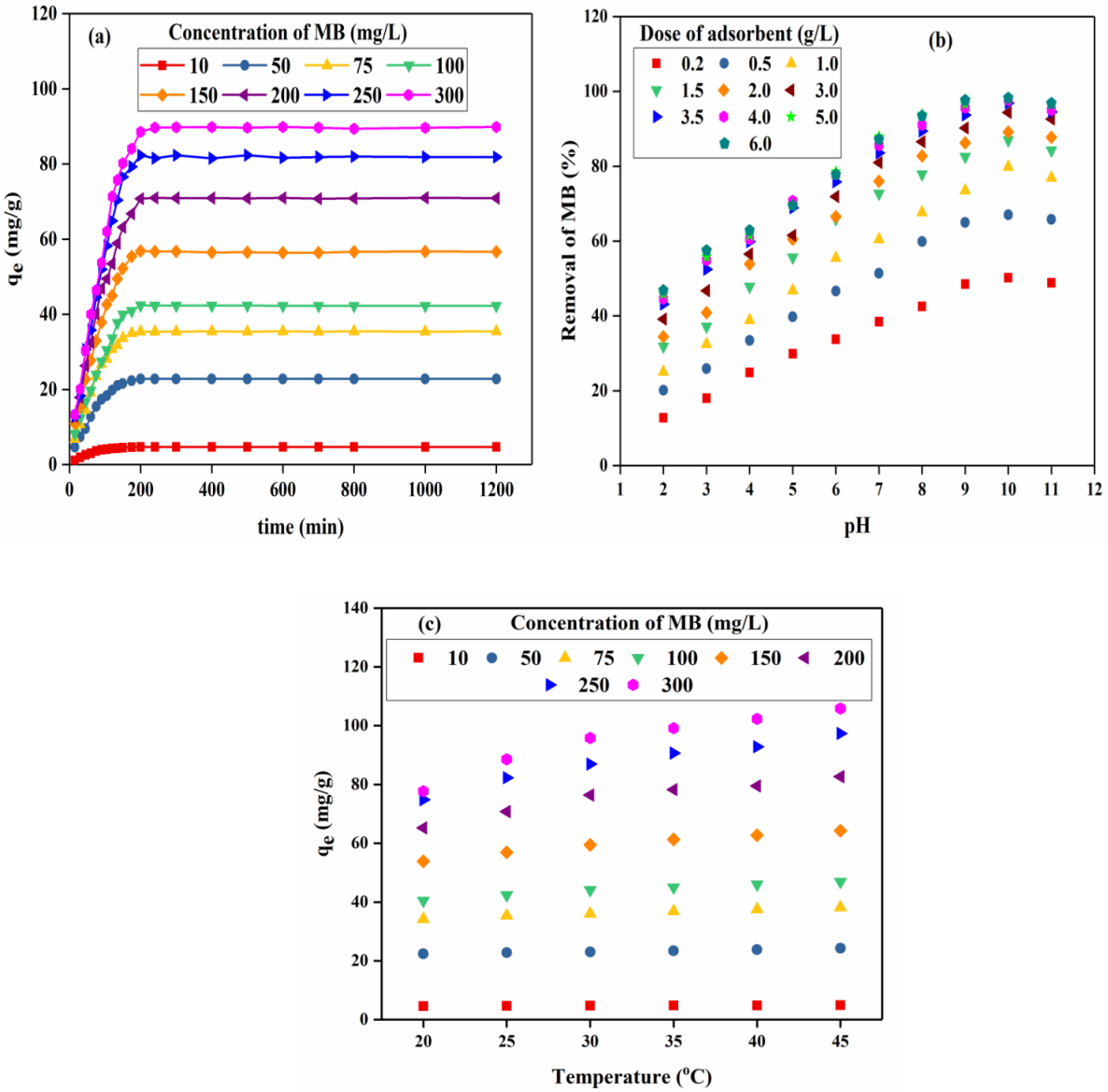

Figure 7.6 Effect of operating parameters on uptake capacity of adsorption process using Biochar-TAN (a) effect of time and concentration (at fixed pH = 10, Temp = 298 K, adsorbent dose = 2 g/L) (b) effect of pH and dose (at fixed Temp = 298 K, MB concentration = 50 mg/L, time = 200 min) (c) effect of temperature and concentration (at fixed pH = 10, adsorbent dose = 2 g/L, time = 200 min)

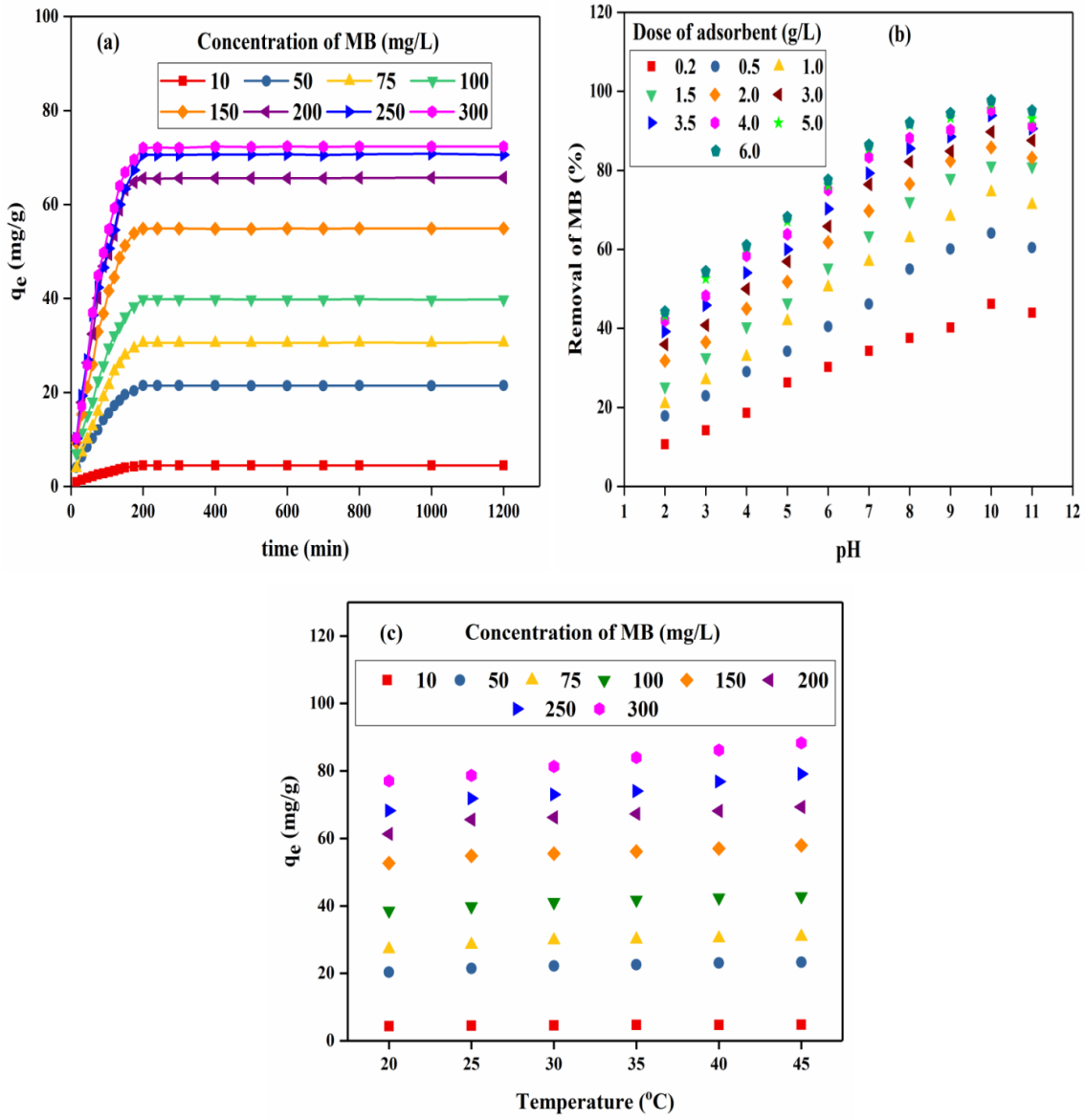

Figure 7.7 Effect of operating parameters on uptake capacity of adsorption process using Biochar-DAN (a) effect of time and concentration (at fixed pH = 10, Temp = 298 K, adsorbent dose = 2 g/L) (b) effect of pH and dose (at fixed Temp = 298 K, MB concentration = 50 mg/L, time = 200 min) (c) effect of temperature and concentration (at fixed pH = 10, adsorbent dose = 2 g/L, time = 200 min)

7.3.2.2 Effect of pH of solution and adsorbent dose

The pH of working solution is a very significant parameter since it affects the charge density and dissociation of functional groups associated with adsorbent as well as structure of MB (Li et al., 2018; Liu et al., 2019). Effect of pH of solution varying from 2.0 to 11.0, for both the biochar (Biochar-TAN and Biochar-DAN) was investigated by different adsorbent dosage varying from 0.2 to 6 g/L for 50 mg/L MB solution and 1200 min adsorption time. The results are displayed in Fig. 7.6(b) and Fig. 7.7(b). It can be perceived at particular dose of adsorbent, the percentage removal increased up to a maximum value at pH 10 and after that percentage removal slightly decreased. Similar finding were also reported by Li et al. (Li et al., 2018), Ji et al. (Ji et al., 2019) for adsorption of MB. The significance of pH can be analyzed based on the pH of solution and point of zero charge for both the adsorbents. MB is accepted as cationic dye having positive charge. The pH_{pzc} for Biochar-DAN and Biochar-TAN was found to be 8.10 and 7.6, respectively. It implies that at pH lower than pH_{pzc}, the adsorbent surface will be positively charged, while, pH greater than pH_{pzc}, it will be negatively charged. Thus, the electrostatic attraction among MB molecules and adsorbent will be stronger at higher pH. However, at pH higher than 10 the steric hindrance among the $-OH^-$ ions might be responsible for reduction in percentage removal of MB.

The adsorbent dose is a crucial parameter for investigating the adsorption capacity of both biochars. The effect of adsorbent dose was examined by changing the adsorbent dose from 0.2 to 6.0 g/L and the results are displayed in Fig. 7.6(b) for Biochar-TAN and Fig. 7.7(b) for Biochar-DAN. It was noticed that as the adsorbent dose increases, the percentage removal of MB for both biochar has increased. This could be attributed to higher surface

area and more number of active adsorption sites with increase in adsorbent dose. However, lower adsorption capacity was noticed at higher adsorbent dose because increase in adsorbent dose, enhance the probability of collision between adsorbent molecules, which resulted in aggregation and overlapping of adsorbent molecules causing lower surface area as well as longer diffusion path for MB molecules (Alinejad-Mir et al., 2018; Ye et al., 2015).

7.3.3 Kinetics and mass transfer study for adsorption of MB onto Biochar-DAN and Biochar-TAN

7.3.3.1 Adsorption kinetics

The adsorption kinetics was performed to investigate the rate of adsorption of MB onto the adsorbent. Also, kinetics of adsorption revealed the rate controlling step as well as mass transfer mechanism associated with movement of molecules of MB from liquid solution to adsorbent surface. For adsorption kinetics, the experiments were performed in time interval of 15-200 min by changing the concentration of MB from 10-300 mg/L and keeping rest of the factor like (pH, adsorbent dose, temperature, and incubator speed) at constant value. In this study, three kinetic models namely, pseudo first order (Eq. 7.3), pseudo second order (Eq. 7.4) and Elovich model (Eq. 7.5) and two mass transfer models such as Weber and Morris (Eq. 7.6) also known as intra-particle diffusion model and Boyd model (Eq. 7.7) were tested.

$$\log(q_e - q_t) = \log q_e - \frac{k_1 t}{2.303} \quad (7.3)$$

$$\frac{t}{q_t} = \frac{t}{q_e} + \frac{1}{k_2 q_e^2} \quad (7.4)$$

$$q_t = \frac{1}{\beta}\ln(\alpha\beta) + \frac{1}{\beta}\ln t \quad (7.5)$$

$$q_t = k_{id}t^{0.5} + C \quad (7.6)$$

$$\ln(1 - F) = -k_{fd}t \quad (7.7)$$

Where q_e is equilibrium uptake capacity (mg/g); q_t is uptake capacity (mg/g) at time t; k_1 is pseudo-first-order rate constant (min^{-1}): k_2 is pseudo-second-order rate constant (g/mg.min); β is constant for desorption (g/mg); α is rate of initial desorption (mg/gmin); k_{id} is rate constant for intra-particle diffusion; C is intercept (mg/g); F is fraction for adsorbed solute at any time t ($F = \frac{q_t}{q_e}$, dimensionless); k_{fd} is constant for liquid film diffusion (sec^{-1}).

The Pseudo first order model was applied to calculate the rate of adsorption of adsorbate onto the surface of adsorbent based on the adsorption capacity. As per the pseudo first order model, initially MB molecules were not present on the surface of adsorbent at the start of adsorption process, however MB molecules start accumulating on the surface of adsorbent until the process reached equilibrium. The theoretical adsorption capacity and rate constant parameters were calculated at different concentrations using Eq. 7.3 and results are shown in Fig. 7.8(a) for Biochar-TAN and Fig. 7.9(a) for Biochar-DAN. The theoretical adsorption capacity ($q_{e,cal}$), first order rate constant (k_1) and correlation coefficient (R^2) for both the biochar are given in Table 5 at different concentrations of MB dye from 10-300 mg/L. The adsorption capacity for Biochar-DAN varies from 5.9563 to 128.9228 mg/g, while, for Biochar-TAN it varies from 5.5195 to 131.492 mg/g, once the concentration varies from 10 to 300 mg/L. The value of k_1 varies from 0.0166 to 0.0244

min^{-1} for Biochar-DAN and for Biochar-TAN it varies from 0.0161 to 0.0234 min^{-1}. R^2 for Biochar-DAN varies from 0.8941 to 0.9629, while for Biochar-TAN it varies from 0.9052 to 0.9876.

The pseudo second order model was employed to describe the dynamics of adsorption process. This model is based on the assumption that chemisorption is the rate determining step and adsorption capacity is proportional to the available active site on the surface of adsorbent. The theoretical adsorption capacity and rate constant parameters were calculated at different concentrations using the Eq. 7.4 and results are shown in Fig. 7.8(b) for Biochar-TAN and Fig. 7.9(b) for Biochar-DAN. The theoretical adsorption capacity ($q_{e,cal}$), pseudo second order rate constant (k_2) and correlation coefficient (R^2) for both the biochar are shown in given in Table 7.5 at different concentrations of MB from 10-300 mg/L. The adsorption capacity for Biochar-DAN varies from 6.4771 to 205.7613 mg/g, while, for Biochar-TAN it varies from 6.4808 to 208.3333 mg/g, once the concentration varies from 10 to 300 mg/L. The value of k_2 varies from 2.33×10^{-3} to 1.96×10^{-5} (g/(mg.min)) for Biochar-DAN and for Biochar-TAN it varies from 2.32×10^{-3} to 1.91×10^{-5} (g/(mg.min)). R^2 for Biochar-DAN varies from 0.9025 to 0.9899, while for Biochar-TAN it varies from 0.8927 to 0.9889. The adsorption affinity or initial rate constant ($V_o= k_2q_e^2$) signifies the rate of adsorption at the beginning. For Biochar-DAN the value of V_o varies from 0.0977 to 0.8479 mg/g.min, while for Biochar-TAN it varies from 0.9744 to 0.8289 mg/g.min. At different concentration of MB dye, the value of k_2 decreased with increase in V_o and $q_{e,cal}$. This revealed that adsorption of MB dye was faster at initial stage when the concentration of MB dye was increased.

Further, Elovich model was also fitted with experimental results. The Elovich model is employed to test the nature of adsorption whether it is physisorption or chemisorption. With the help of Eq. 7.5 the kinetic parameters α and β are calculated and the results are shown in Fig. 7.8(c) for Biochar-TAN and Fig. 7.9(c) for Biochar-DAN. The value of α for Biochar-DAN varies from 0.2597 to 4.0820, while for Biochar-TAN it varies from 0.8862 to 3.8928. The value of β varies from 0.0675 to 1.1164 for Biochar-DAN, while it varies from 0.0512 to 1.3239 for Biochar-TAN. The value of correlation coefficient for Biochar-DAN varies from 0.7811 to 0.8275, while for Biochar-TAN it varies from 0.7385 to 0.8231.

The kinetic model which gives the closest value of experimental and theoretical adsorption capacity along with correlation value nearer to one will be followed during adsorption process. Based on the above criteria it was found that among the tested models the pseudo second order kinetic model was followed during adsorption for both Biochar-DAN and Biochar-TAN as an adsorbent.

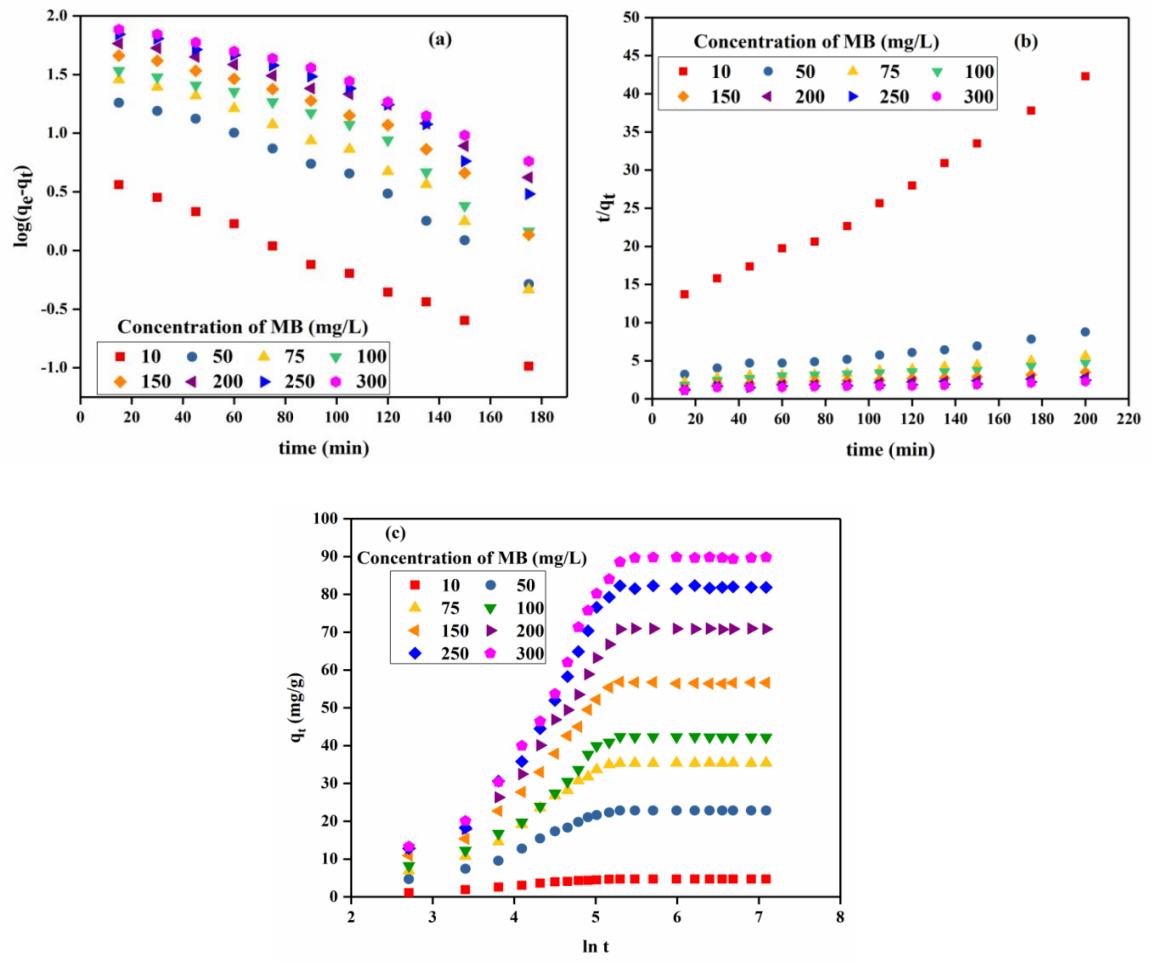

Figure 7.8 Kinetic model for adsorption of MB dye on Biochar-TAN (a) pseudo-first-order (b) pseudo-second-order and (c) Elovich

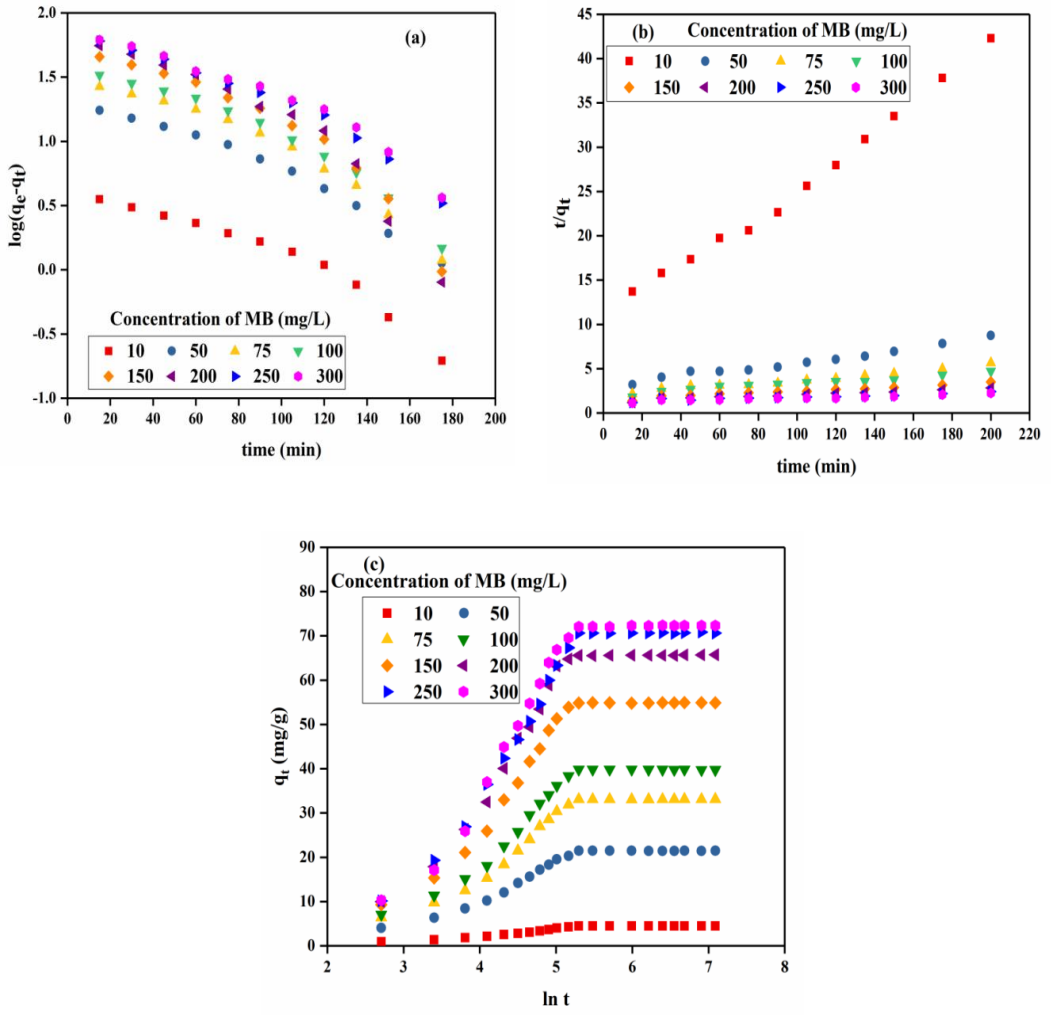

Figure 7.9 Kinetic model for adsorption of MB dye on Biochar-DAN (a) pseudo-first order (b) pseudo-second-order and (c) Elovich

Table 7.5 Adsorption kinetics and related parameters for adsorption of MB dye onto Biochar-DAN and Biochar-TAN

Kinetic model	Parameters	Initial concentration (mg/L)							
		10	50	75	100	150	200	250	300
Biochar-DAN									
Pseudo first order	$q_{e,exp}$(mg/g)	4.4755	21.47	30.588	39.835	54.855	65.58	70.6125	72.075
	$q_{e,cal}$ (mg/g)	5.9563	28.5121	48.8742	59.5634	95.2796	128.9228	94.7850	97.1627
	k_1 (min^{-1})	0.0166	0.0169	0.0186	0.0166	0.0217	0.0244	0.0169	0.0162
	R^2	0.9181	0.9629	0.9402	0.9181	0.9181	0.8941	0.9549	0.9453
Pseudo second order	$q_{e,cal}$ (mg/g)	6.4771	36.9003	60.0240	76.3358	102.3540	131.5789	187.9699	205.7613
	k_2 (g/(mg.min))	2.33×10^{-3}	2.45×10^{-4}	1.34×10^{-4}	8.57×10^{-5}	6.43×10^{-5}	4.45×10^{-5}	2.24×10^{-5}	1.96×10^{-5}
	V_o (mg/g.min)	0.0977	0.3335	0.4827	0.4993	0.6704	0.7704	0.8479	0.8298
	R^2	0.9899	0.9758	0.9695	0.9492	0.9637	0.9526	0.9025	0.9190
Elovich model	β (g/mg)	1.1164	0.2313	0.1493	0.1230	0.0902	0.0759	0.0688	0.0675
	α (mg/g.min)	0.2597	1.2437	1.8923	2.2012	3.2549	4.0820	3.8096	4.0128
	R^2	0.8275	0.8137	0.8048	0.8060	0.7913	0.7811	0.8189	0.7910
Biochar-TAN									
Pseudo first order	$q_{e,exp}$(mg/g)	4.732	22.835	35.404	42.305	56.7225	70.98	81.525	89.67
	$q_{e,cal}$ (mg/g)	5.5195	33.9859	60.2282	65.9629	88.920	92.755	131.492	125.545
	k_1 (min^{-1})	0.0212	0.2180	0.0234	0.0197	0.0198	0.0156	0.0188	0.0161
	R^2	0.9876	0.9650	0.9177	0.9192	0.9052	0.9517	0.9228	0.9601
Pseudo second order	$q_{e,cal}$ (mg/g)	6.4808	36.9003	60.2409	76.3358	103.0927	131.5789	188.6792	208.3333
	k_2 (g/(mg.min))	2.32×10^{-3}	2.45×10^{-4}	1.33×10^{-4}	8.57×10^{-5}	6.34×10^{-5}	4.45×10^{-5}	2.22×10^{-5}	1.91×10^{-5}
	V_o (mg/g.min)	0.9744	0.3335	0.4826	0.4993	0.6738	0.7704	0.7903	0.8289
	R^2	0.9889	0.9761	0.9664	0.9441	0.9601	0.9479	0.8927	0.9109
Elovich model	β (g/mg)	1.3239	0.2382	0.1501	0.1176	0.0883	0.0677	0.0573	0.0512
	α (mg/g.min)	0.8862	2.0813	2.9287	2.5007	3.4518	3.5466	3.8928	3.8371
	R^2	0.7385	0.7673	0.7684	0.7967	0.7981	0.8231	0.7991	0.8174

7.3.3.2 Mass transfer models

7.3.3.2.1 Weber and Morris model

Weber and Morris model was employed to investigate whether the rate controlling step during the adsorption process was film diffusion or intra- particle diffusion (Fan et al., 2017). Fig. 7.10(a) and Fig. 7.11(a) showed the intra-particle diffusion model at different concentration of MB solution ranging from 10 to 300 mg/L for Biochar-TAN and Biochar-DAN respectively. The value of k_{id} and correlation coefficient obtained from the plot are given in Table 7.6. It can be seen that k_{id} value increased with increase in concentration due to higher driving force for adsorption. However, significant increase in k_{id} value was observed up to 150 mg/L and after that minor increase in k_{id} value was observed. This might be due to saturation of adsorbent surface at higher concentration of MB. Also, k_{id} value was higher in case of Biochar-TAN as compared to Biochar-DAN, which can be inferred to faster adsorption rate in case of Biochar-TAN than the Biochar-DAN. In addition, it was found that for both the biochar, the adsorption process was controlled by three stages. In first stage, initial adsorption was controlled by external surface adsorption. The intra-particle diffusion was rate determining step in second stage where gradual adsorption takes place. The third stage of adsorption was associated with final equilibrium stage where intra-particle diffusion gradually slows down due to lower concentration of MB (Wang et al., 2018a). In addition, for each concentration, none of the lines passes through origin, which confirmed that adsorption process was not exclusively governed by internal diffusion, however some other factors such as external diffusion or ion exchange might be responsible for adsorption process.

7.3.3.2.2 Boyd model

Further, Boyd model was also studied to investigate whether external film or internal diffusion controlled the adsorption of MB onto biochar. The Boyd plots for Biochar-TAN and Biochar-DAN at different concentration (10-300 mg/L) are shown in Fig. 7.10(b) and Fig. 7.11(b) respectively. The plots between ln(1-F) and time were used to calculate k_{fd} at different concentrations. The value of k_{fd} and correlation coefficients are presented in Table 7.6. The correlation coefficient for Biochar-TAN varied from 0.9137 to 0.988 and for Biochar-DAN it varied from 0.8940 to 0.9688. For both the biochar (Biochar-DAN and Biochar-TAN) the Boyd plots were non-linear at different concentrations, and did not pass through origin and revealing that it was not only intra-particle diffusion that determined the rate determining factor for adsorption of MB onto biochar. A combined effect of external surface diffusion, intra-particle diffusion and chemical reactions might be responsible for adsorption process.

Table 7.6 Mass transfer models and related parameters for adsorption of MB dye onto Biochar-DAN and Biochar-TAN

	Mass transfer parameters					
	Weber and Morris model			Boyd Model		
C_o (mg/L)	k_{id} (mg/g.min$^{1/2}$)	R^2	C_1 (intercept)	k_{fd} (sec^{-1})	R^2	C_2 (intercept)
Biochar-DAN						
10	0.1018	0.6004	1.9436	0.0165	0.9197	0.2813
50	0.4864	0.5781	9.4275	0.0169	0.9688	0.2836
75	0.7531	0.5709	14.4950	0.0186	0.9406	0.3888
100	0.9123	0.5696	17.2737	0.0182	0.9438	0.3745

150	1.2315	0.5483	24.6453	0.0217	0.9086	0.5521
200	1.4504	0.5324	30.1752	0.0244	0.8941	0.6759
250	1.6275	0.5770	30.4271	0.0168	0.9549	0.2944
300	1.6454	0.5432	31.9215	0.0196	0.9669	0.4135
Biochar-TAN						
10	0.7553	0.7385	0.1208	0.0213	0.9888	0.1541
50	4.1977	0.7673	−2.9453	0.0218	0.9685	0.3978
75	6.6578	0.7684	−5.4718	0.0238	0.9208	0.5496
100	8.5032	0.7967	−10.4071	0.0199	0.9260	0.4526
150	11.3130	0.7981	−13.4410	0.0200	0.9137	0.4526
200	14.7700	0.8231	−21.0720	0.0158	0.9526	0.2673
250	17.4330	0.7991	−26.1550	0.0204	0.9156	0.5390
300	19.5140	0.8174	−31.7550	0.0165	0.9633	0.3409

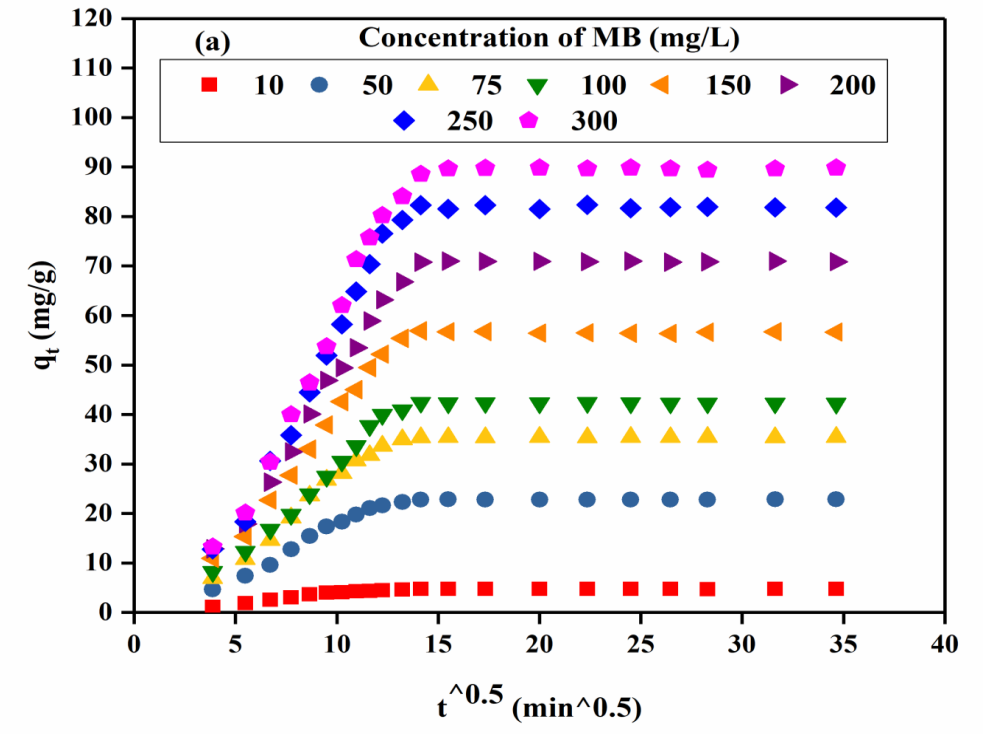

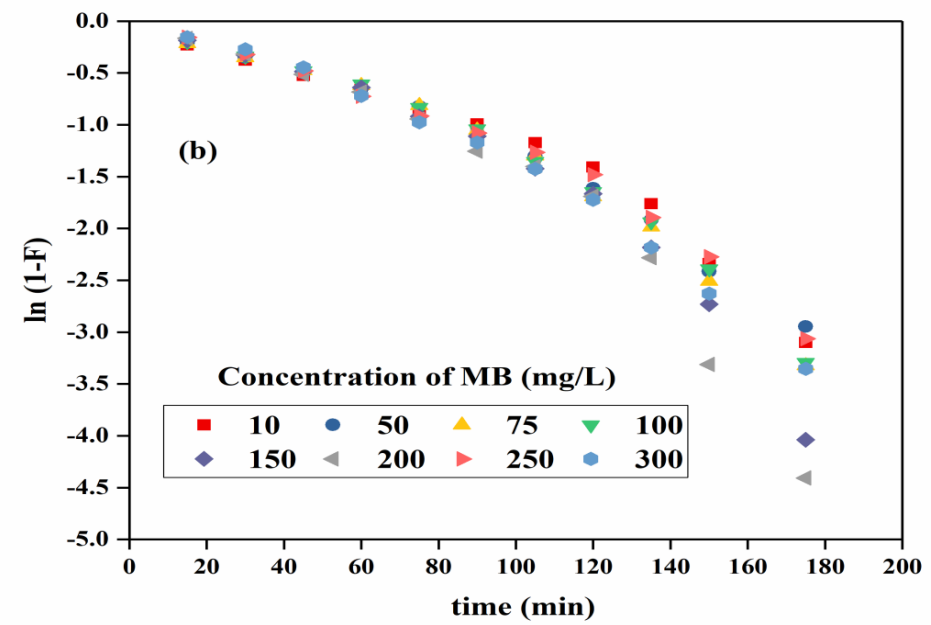

Figure 7.10 Mass transfer model for adsorption of MB dye on Biochar-TAN (a) Weber and Morris model (b) Boyd model

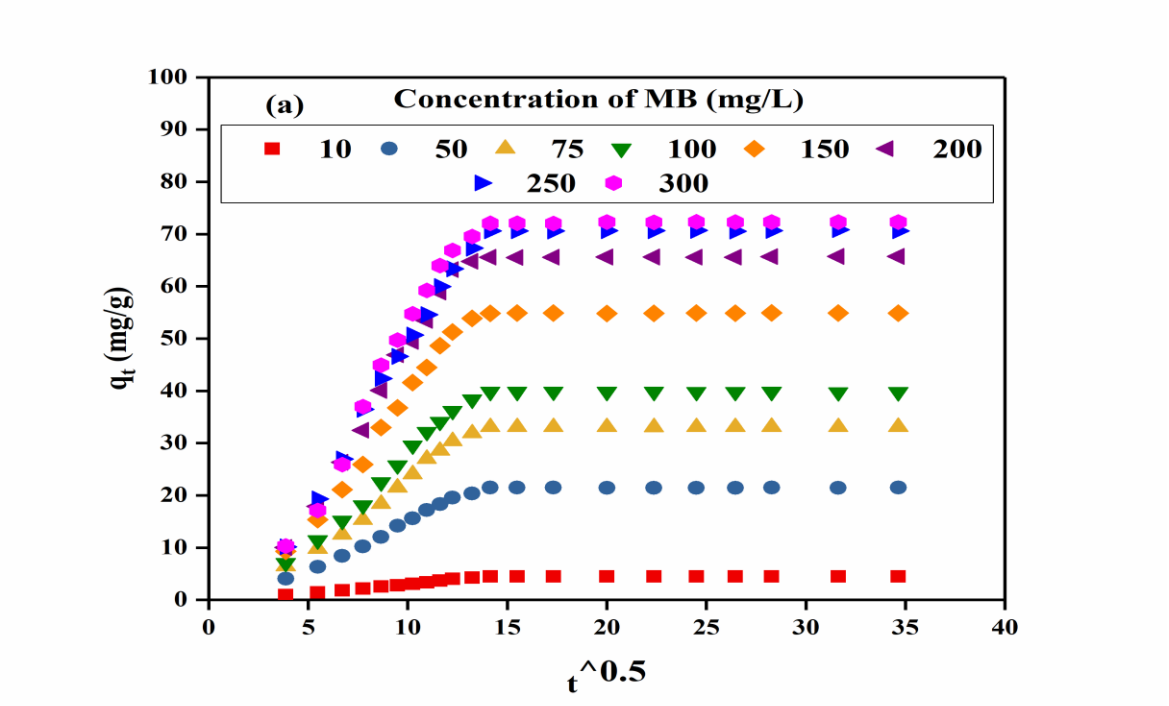

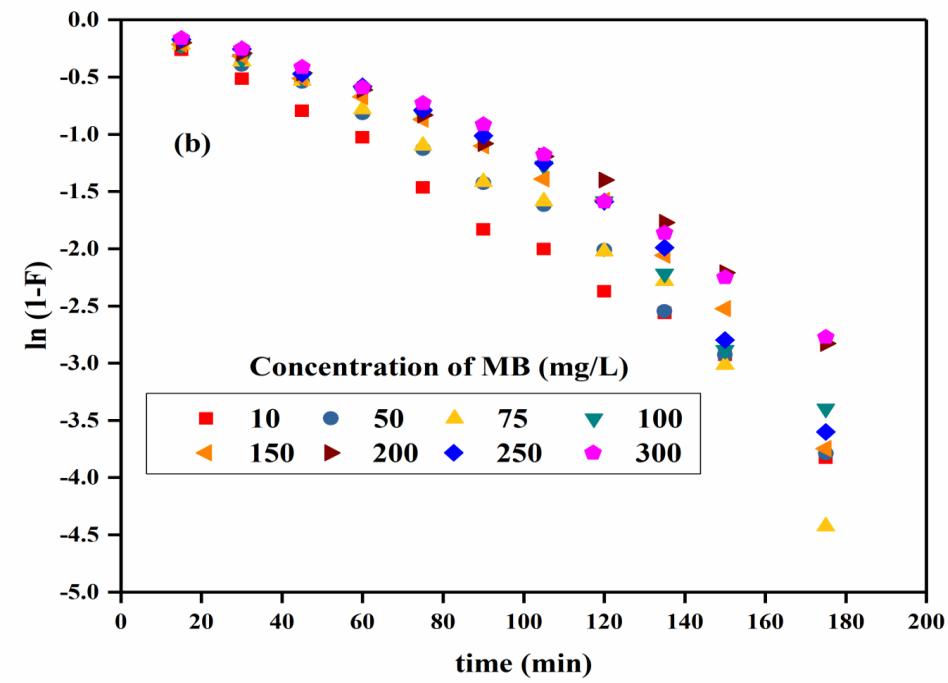

Figure 7.11 Mass transfer model for adsorption of MB dye on Biochar-TAN (a) Weber and Morris model (b) Boyd model

7.3.4 Effect of temperature and isotherms for adsorption of MB onto Biochar-DAN and Biochar-TAN

It is well understood that adsorption is a temperature dependent process. The temperature was varied from 20 to 45 ℃ and adsorption capacity with respect to temperature at different concentration of MB (10-300 mg/L) for Biochar-TAN is shown in Fig. 7.6(c) and for Biochar-DAN is shown in Fig. 7.7(c). At a particular concentration, increase in adsorption capacity is observed with increase in temperature. This might be due to higher mobility of ions at higher temperature and also higher degree of diffusion of MB molecules to the external surface and internal pores of the adsorbent (Saini et al., 2018). Thus, higher

temperature favors the removal of MB (Huang et al., 2019), though the influence of temperature at lower adsorbate concentration was insignificant.

Further, to unveil the adsorption mechanism and distribution of MB in liquid and solid biochar (Biochar-DAN and Biochar-TAN) at equilibrium condition, the adsorption isotherms were fitted with experimental results. In the present study four isotherms namely, Langmuir, Freundlich, Temkin and Sips were fitted with experimental results from both the biochars. The linear and non-linear forms of equations for all the isotherms are given in Table 7.7. The results are shown in Fig. 7.12 for Biochar-TAN and Fig. 7.13 for Biochar-DAN. The parameters calculated for isotherms are presented in Table 7.8. The Langmuir isotherm illustrates the single layer adsorption on specific site of homogeneous surface of adsorbent (Sangon et al., 2018). This model assumes that energy of adsorption is uniform on the surface of adsorbent and no interaction exists between the adsorbed molecules (Saini et al., 2018). The Freundlich isotherm demonstrates the multilayer adsorption process for a heterogeneous surface (Prajapati & Mondal, 2019). Temkin and Pyzhev considered that as a result of adsorbate and adsorbent interaction, the heat associated with adsorption decreased linearly with layer of adsorbed molecules, while, activation energy got distributed homogeneously (Prajapati & Mondal, 2019). The Sips isotherm is derived as a combination and based on limiting behavior of both Langmuir and Freundlich isotherms (Shahryari et al., 2010; Vargas et al., 2011). The maximum adsorption capacity of Biochar-DAN and Biochar-TAN at temperature from 293-318 K was found to be 83.530-89.167 mg/g and 85.959-107.347 mg/g, respectively at fixed concentration of MB dye (50 mg/L) and adsorbent dose (2 g/L). The correlation coefficient (R^2) for Langmuir, Freundlich, Temkin and Sips model for Biochar-TAN was varied between (0.9662-0.9810), (0.9260-

0.9614), (0.9212-0.9500), and (0.9737-0.9818), respectively. And, for Biochar-TAN the value of correlation coefficient varied from (0.9499-0.9822), (0.9765-0.9873), (0.9103-0.9629), and (0.9904-0.9943) for Langmuir, Freundlich, Temkin and Sips model, respectively. Thus, based on the correlation coefficient (R^2), Sips model was found to be followed during adsorption of both Biochar-DAN and Biochar-TAN. The maximum adsorption capacity for both biochar (Biochar-DAN and Biochar-TAN) was found to be 98.2174, and 158.131 mg/g, respectively. The comparable results were also obtained in case of various adsorbents used for removal of MB from aqueous solution (Ji et al., 2019), (Saini et al., 2018), (Liu et al., 2018).

Table 7.7 Linear and non-linear forms of isotherms

Isotherm models	Equation in Nonlinear form	Equation in Linear form	Equation No.
Langmuir isotherm	$q_e = \frac{q_m K_L C_e}{1 + K_L C_e}$	$\frac{C_e}{q_e} = \frac{C_e}{q_m} + \frac{1}{q_m K_L}$ $R_L = \frac{1}{1 + K_L C_O}$	7.8 7.9
Freundlich isotherm	$q_e = K_f C_e^{\frac{1}{n}}$	$\ln q_e = \ln K_f + \frac{1}{n} \ln C_e$	7.10
Temkin isotherm	$q_e = B * \ln(AC_e)$	$q_e = B \ln A + B \ln C_e$ $B (= \frac{RT}{b})$	7.11
Sips isotherm	$q_e = \frac{Q_m (K_s C_e)^{m_s}}{1+(K_s C_e)^{m_s}}$	$\frac{1}{q_e} = \frac{1}{q_m K_s} \left(\frac{1}{C_e}\right)^{1/n} + \frac{1}{q_m}$	7.12

q_e is experimental adsorption capacity (mg/g) at equilibrium; q_m is the maximum adsorption capacity (mg/g) of biochar; K_L is Langmuir constant (L/g); C_e is equilibrium concentration (mg/L) of MB dye in liquid phase; C_o is the initial MB concentration (mg/L); K_f is Freundlich model constant; 1/n is heterogeneity factor constant; R is universal gas constant; T is temperature (K); A is equilibrium binding constant (L/mg); B is Temkin constant associated with enthalpy of adsorption; b is Temkin isotherm constant; K_s and m_s are sips parameters

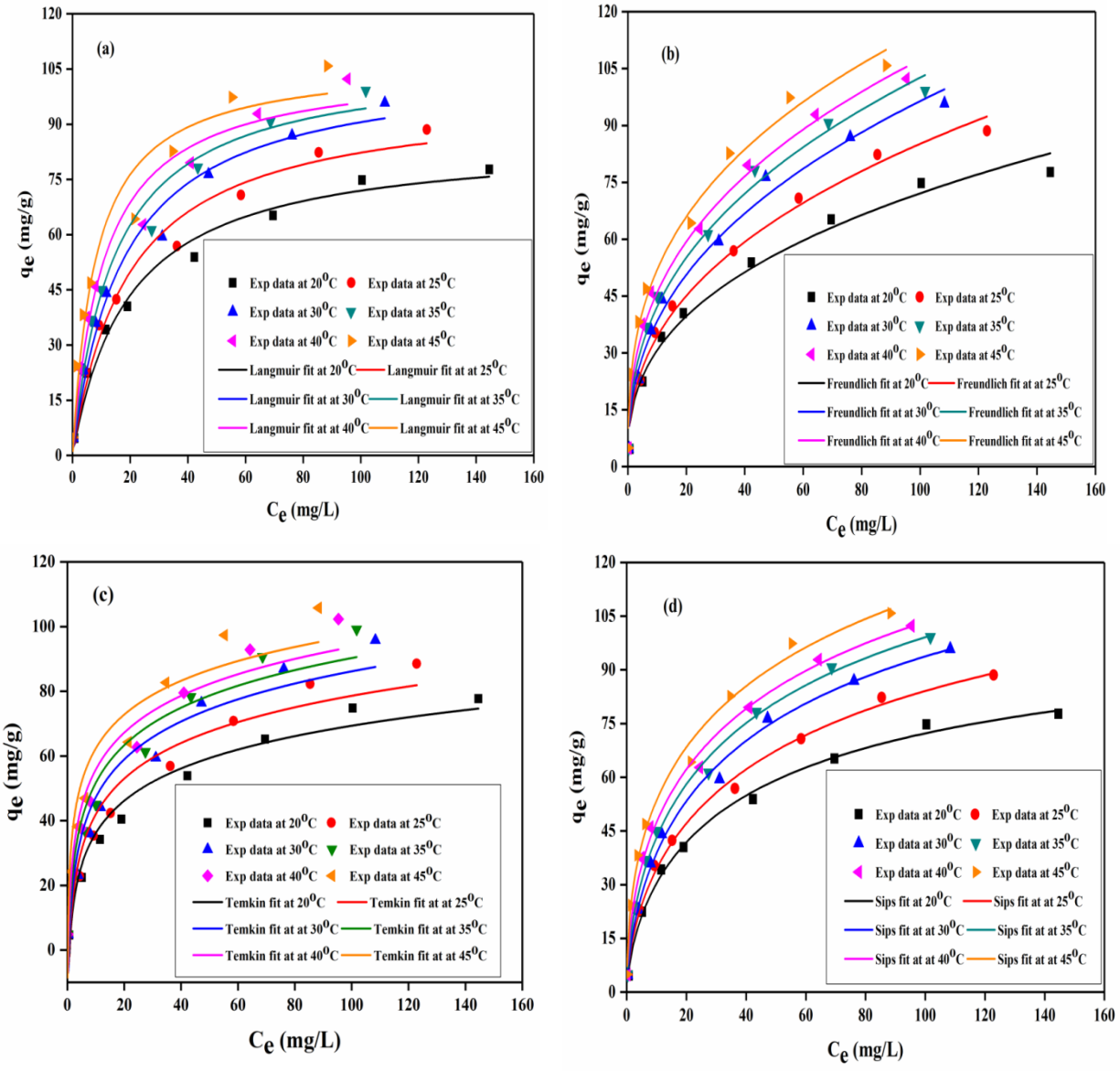

Figure 7.12 Adsorption isotherms for adsorption of MB dye on Biochar-TAN (a) Langmuir isotherm (b) Freundlich isotherm (c) Tempkin isotherm (d) Sips isotherm

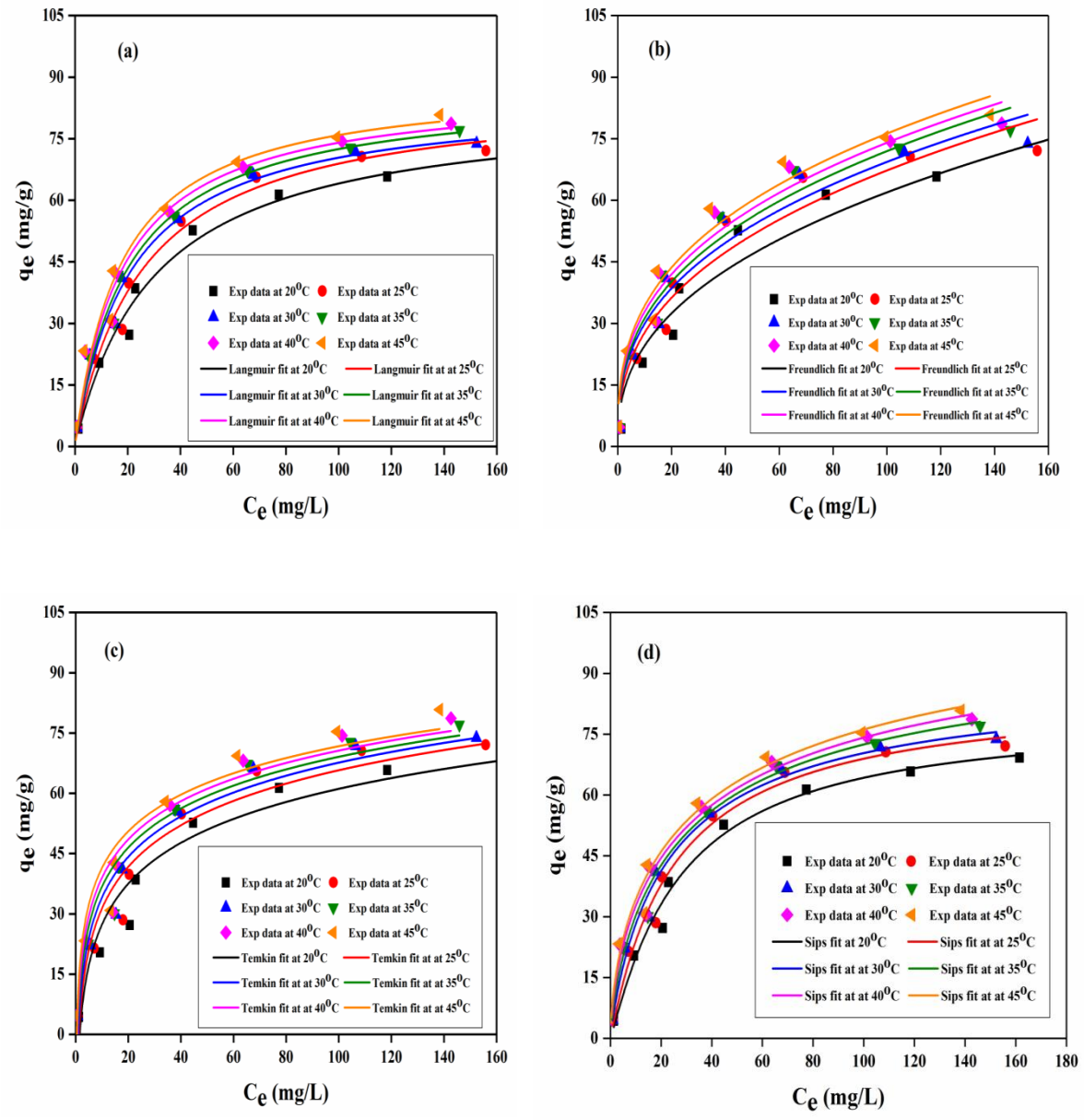

Figure 7.13 Adsorption isotherms for adsorption of MB dye on Biochar-DAN (a) Langmuir isotherm (b) Freundlich isotherm (c) Tempkin isotherm (d) Sips isotherm

Table 7.8 Isotherm and related parameters for adsorption of MB dye onto Biochar-DAN and Biochar-TAN

Isotherm model	Parameters	Temperature (K)					
		293	298	303	308	313	318
Biochar-DAN							
Langmuir	q_m (mg/g)	83.530	86.703	85.165	87.081	87.612	89.167
	K_L (L/mg)	0.0329	0.0387	0.0475	0.0495	0.0544	0.0570
	R_L	0.3780	0.3407	0.2962	0.2877	0.2688	0.2597
	R^2	0.9810	0.9794	0.9837	0.9777	0.9662	0.9651
Freundlich	K_f	9.7477	11.4698	12.923	13.546	14.595	15.428
	n	2.491	2.6037	2.741	2.7577	2.836	2.880
	R^2	0.9312	0.9260	0.9390	0.9527	0.9549	0.9614
Temkin	B	14.6782	14.9444	14.5848	14.0513	13.7453	13.1675
	A (L/mg)	0.6428	0.8134	1.0333	1.3648	1.7033	2.3185
	R^2	0.9324	0.9320	0.9500	0.9375	0.9356	0.9212
Sips	q_m (mg/g)	79.906	85.689	90.091	100.9544	111.230	119.7011
	K_S	0.0363	0.0397	0.0414	0.0333	0.0239	0.0239
	m_s	0.9141	0.9757	1.1188	1.2917	1.5627	1.5627
	R^2	0.9779	0.9753	0.9818	0.9794	0.9737	0.9756
Biochar-TAN							
Langmuir	q_m (mg/g)	85.959	98.2174	106.509	107.651	106.351	107.3474
	K_L (L/mg)	0.0113	0.0515	0.0567	0.0695	0.0913	0.1229
	R_L	0.6389	0.2797	0.2607	0.2234	0.1796	0.1399
	R^2	0.9822	0.9770	0.9799	0.9746	0.9653	0.9499
Freundlich	K_f	13.03	13.77	15.24	17.32	19.65	23.47
	n	2.692	2.528	2.497	2.588	2.711	2.902
	R^2	0.9765	0.9860	0.9841	0.9855	0.9870	0.9873
Temkin	B	124.428	15.931	16.934	16.772	16.472	15.102
	A (L/mg)	1.222	1.388	1.620	2.175	2.950	6.185
	R^2	0.9629	0.9420	0.9294	0.9283	0.9328	0.9103
Sips	q_m (mg/g)	114.654	158.131	162.189	176.5597	199.38	241.4263
	K_S	0.0220	0.0123	0.0163	0.0151	0.0114	0.0069
	m_s	1.4823	1.6345	1.5654	1.6763	1.8607	2.1209
	R^2	0.9943	0.9942	0.9935	0.9936	0.9922	0.9904

7.3.5 Thermodynamic parameters for adsorption of MB onto Biochar-DAN and Biochar-TAN

The thermodynamic parameters for adsorption of MB onto Biochar-DAN and Biochar-TAN at equilibrium were calculated at different temperature ranging from 20-45 ℃ keeping rest of the parameters constant. The Gibb's free energy (ΔG^o), Entropy (ΔS^o) and Enthalpy (ΔH^o) were calculated using Eqs. (7.13)-(7.16) (Saini et al., 2018).

$$\Delta G^o = -RT \ln K_o \quad (7.13)$$

$$K_o = \frac{C_{ad,eq}}{C_{eq}} \quad (7.14)$$

$$\Delta G^o = \Delta H^o - T\Delta S^o \quad (7.15)$$

$$\ln K_o = -\frac{\Delta H^o}{RT} + \frac{\Delta S^o}{R} \quad (7.16)$$

where ΔG^o (kJ/mol), ΔS^o (J/mol.K) and ΔH^o (kJ/mol) are the change in Gibbs free energy, entropy and enthalpy, respectively. T, R and K_o are temperature (K), universal gas constant (8.314 J/mol.K) and the equilibrium constant, respectively. $C_{ad,eq}$ (mg/L) is the amount of MB on the surface of adsorbent at equilibrium. C_{eq} (mg/L) is the equilibrium concentration of dye in the solution.

The values of ΔG^o, ΔS^o and ΔH^o are obtained from the slope and intercept of the van't Hoff plot between $\ln K_o$ versus (1/T). The results are shown in Fig. 7.14(a) and (b) for Biochar-TAN and Biochar-DAN, respectively. The value of ΔG^o, ΔS^o and ΔH^o for both the biochar are listed in Table 7.9. The negative value of Gibbs free energy at different temperature for both the biochar confirmed that the adsorption process is spontaneous and feasible in

nature (Ji et al., 2019). Also, decrease in ΔG^o with temperature revealed that higher temperature favors the adsorption process. The positive values of enthalpy at different temperature indicate that adsorption process is endothermic in nature. The positive value of entropy at different temperature suggested that the randomness at solid/liquid interface during the adsorption process increases (Fan et al., 2017). In addition, lower value of ΔG^o for Biochar-TAN as compared to Biochar-DAN indicates its suitability as an adsorbent for removal of aqueous MB.

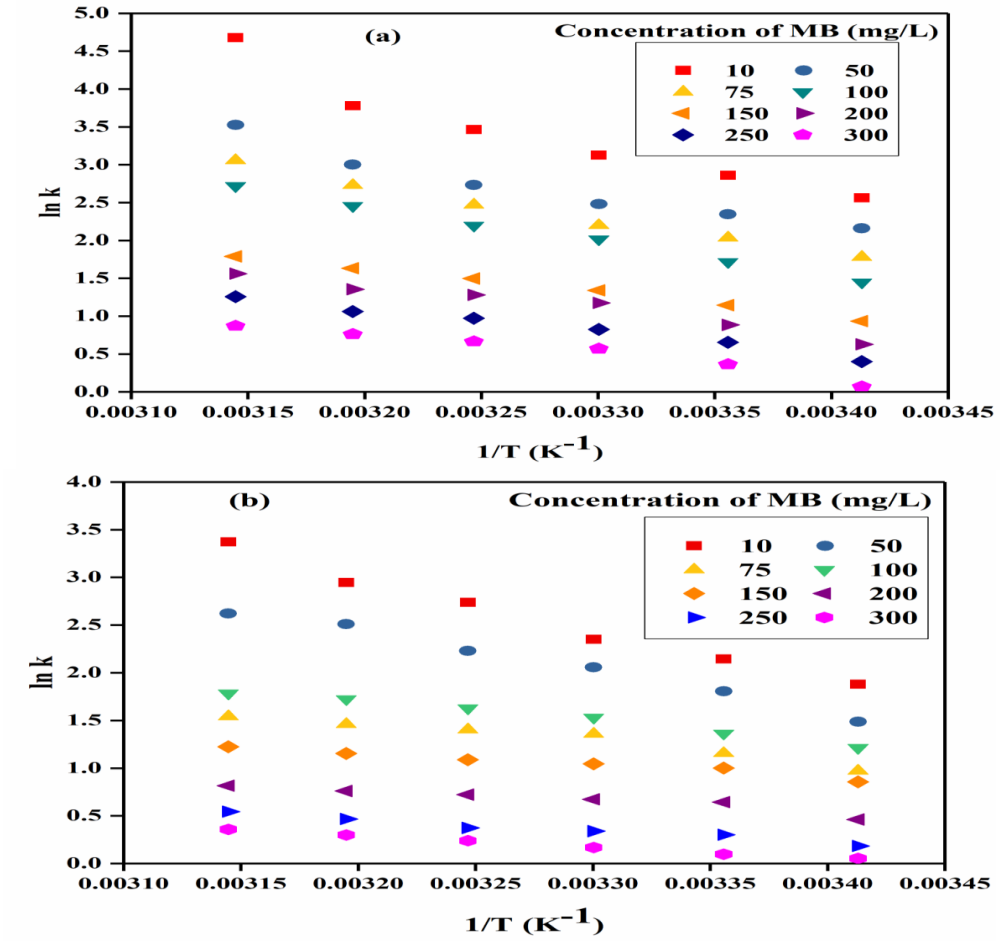

Figure 7.14 van't Hoff plot (a) Biochar-TAN (b) Biochar-DAN

Table 7.9 Thermodynamic parameters for adsorption of MB dye onto Biochar-DAN and Biochar-TAN

Parameters				Temperature (K)					
				293	298	303	308	313	318
C_o (mg/L)	ΔH^o (kJ/mol)	ΔS^o (J/mol.K)	R^2	ΔG^o (kJ/mol)					
Biochar-DAN									
10	45.267	169.672	0.9853	-4.582	-5.312	-5.925	-7.010	-7.668	-8.914
50	35.275	133.173	0.9886	-3.625	-4.473	-5.186	-5.707	-6.534	-6.929
75	16.983	66.571	0.9304	-2.367	-2.863	-3.423	-3.595	-3.799	-4.078
100	17.915	71.509	0.9790	-2.959	-3.384	-3.858	-4.173	-4.490	-4.721
150	10.380	42.834	0.9624	-2.087	-2.482	-2.634	-2.787	-3.005	-3.237
200	9.659	37.294	0.8975	-1.125	-1.597	-1.696	-1.849	-1.979	-2.158
250	10.306	36.827	0.9701	-0.450	-0.748	-0.857	-0.956	-1.217	-1.440
300	9.728	33.558	0.9954	-0.133	-0.243	-0.426	-0.614	-0.780	-0.949
Biochar-TAN									
10	60.267	225.798	0.9100	-6.242	-7.084	-7.878	-8.875	-9.838	-12.371
50	39.785	152.849	0.9171	-5.264	-5.815	-6.254	-6.996	-7.814	-9.320
75	38.619	146.292	0.9843	-4.336	-5.044	-5.541	-6.328	-7.105	-8.083
100	38.823	144.580	0.9966	-3.527	-4.255	-5.084	-5.629	-6.395	-7.196
150	26.147	97.214	0.9952	-2.278	-2.836	-3.379	-3.833	-4.252	-4.732
200	27.489	99.596	0.9531	-1.530	-2.192	-2.961	-3.281	-3.529	-4.129
250	25.107	89.416	0.9761	-0.971	-1.626	-2.081	-2.487	-2.761	-3.328
300	23.578	81.830	0.9367	-0.175	-0.906	-1.437	-1.709	-1.987	-2.310

7.3.6 Possible mechanism for adsorption of MB onto biochars

The adsorption of MB onto biochar is a complex process where multiple phenomenon such as electrostatic attraction, hydrogen bonding, ion exchange, π-π interaction, etc. might be responsible for adsorption process (Fan et al., 2016). The electrostatic attraction occurs as a result of change of pH during the adsorption process (Fan et al., 2017). With increase in

pH, the increase in $-OH^-$ ions in the solution increases the electrostatic attraction force between cationic MB dye (Chen et al., 2019). However, at pH higher than 10 the steric hindrance among the $-OH^-$ ions might reduce the rate of adsorption. The results of kinetics showed that the adsorption of MB onto biochars occurred through physical surface attraction and chemical bonding. Mainly, adsorption of MB proceeds by three steps: (1) diffusion of MB molecules through liquid film surrounding the adsorbent, (2) adsorption of MB molecules on the surface of adsorbent and (3) intra-particle diffusion of MB molecules in-side the pores of adsorbent. The schematic of possible pathways for adsorption of MB is depicted in Fig. 7.15. The FTIR and SEM-EDX analyses revealed the occurrence of -N-H and Si-O-Si functional groups present on the surface of biochar. These groups may contribute in adsorption process MB dye onto biochar through hydrogen bonding and π-π interaction. The inter-molecular hydrogen bond may be formed between nitrogen present in MB dye and hydrogen present on biochar. The inter-molecular hydrogen bonds are associated with adsorption processes and are categorized by means of non-electrostatic attraction (Fan et al., 2017). The –Si-O-Si groups and phenolic sites present on to biochar may participate in adsorption process through π-π interaction. In addition, ion exchange and surface complexation on the surface of biochar might be important mechanism involved during adsorption process. XRD analysis revealed that SiO2, CaO, MgO, $CaCO_3$, and $Ca(OH)_2$ were associated with the surface of biochar which might be proficient physical adsorption spot for the dye molecules (Chen et al., 2019). Comparing the Biochar-TAN and Biochar-DAN, the ion exchange and surface complexation was noteworthy in case of Biochar-TAN as compared to Biochar-DAN. This might be due to significant occurrence of SiO_2, CaO, MgO, $CaCO_3$, and $Ca(OH)_2$ on the surface of Biochar-TAN as

revealed by XRD analysis. Similar results for adsorption mechanism of MB dye onto biochar were also reported in many literatures (Jin et al., 2015; Shi et al., 2014; Sun et al., 2013).

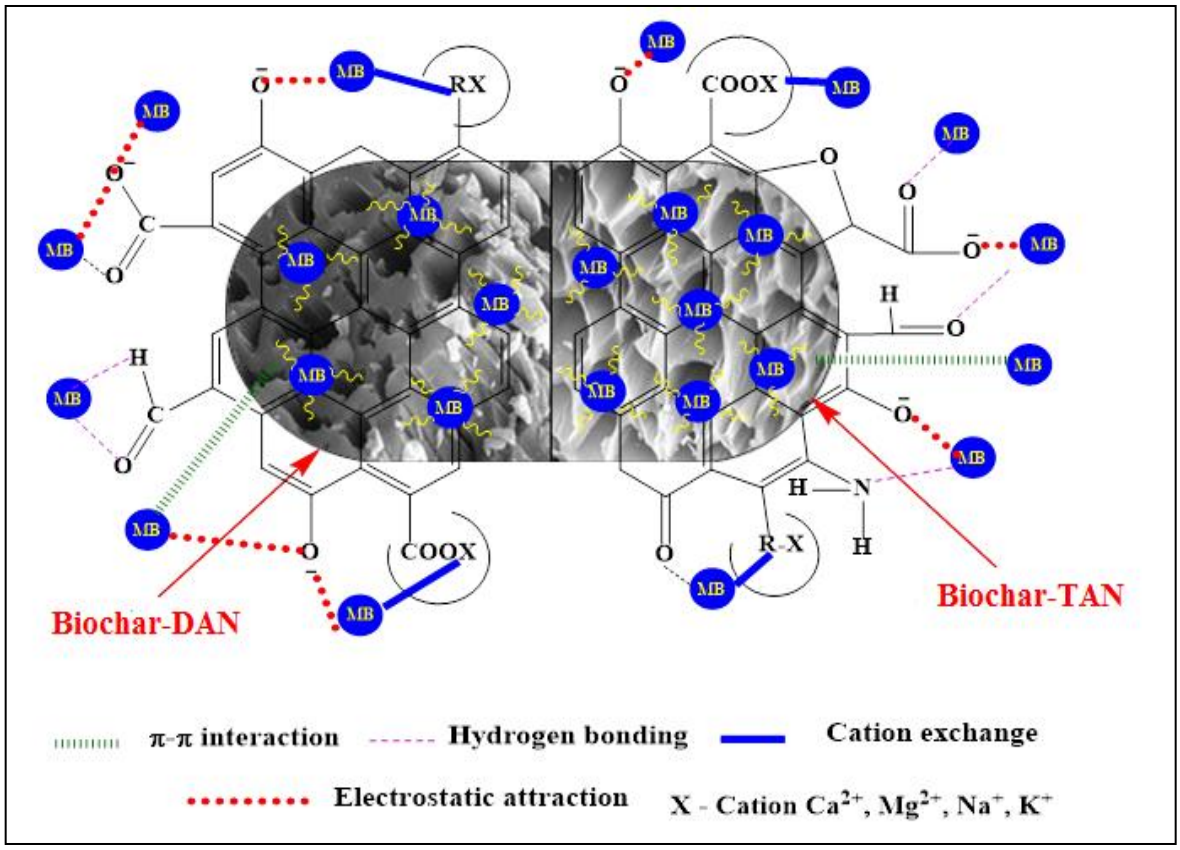

Figure 7.15 Possible mechanisms for adsorption of MB onto biochar

7.4 Conclusions

A comparative study was performed for removal of methylene blue dye from aqueous solution using biochar obtained from pyrolysis of DAN and TAN as an adsorbent. The FTIR analysis showed the decrease in intensity and shifting of peaks which illustrates the

adsorption of MB onto both biochar. The BET surface area of Biochar-DAN and Biochar-TAN was found to be 80.40 and 103.47 m^2/g, respectively, and both biochar can be classified as mesoporous material. The void pores and honey comb like structure of biochar was also revealed by SEM analysis. The maximum adsorption capacity for Biochar-TAN was 158.13 mg/g, while, for Biochar-DAN it was 85.68 mg/g. The higher adsorption capacity of Biochar-TAN towards MB removal was due to higher surface area, pore volume and surface complexation as compared to Biochar-DAN. The Sips isotherm model was best fitted to the experimental results for both biochar as compared to Langmuir, Freundlich and Temkin model. This showed that Langmuir model was followed at lower concentration, while, Freundlich model was followed at higher concentration of MB. The kinetic study for adsorption showed that the pseudo-second-order kinetic model best described the adsorption process of MB dye onto biochar revealing that diffusion through liquid film, adsorption at surface and intra-particle diffusion might be the rate-determining step during adsorption of MB. Additionally, mass transfer studies revealed that both film diffusion and intra-particle diffusion was the rate determining step. The thermodynamic study showed that adsorption of MB onto biochar was endothermic and spontaneous in nature. Further, it was found that four kind of interaction between MB dye and adsorbent were mainly responsible for adsorption process namely, electrostatic attraction, hydrogen bonding, ion exchange and surface complexation and π- π interaction.